Supplementary Information (SI) for Green Chemistry.

# Supporting Information

## 3D printed, metal-free, carbon-based catalytic electrode for converting of $CO_2$ into syngas

Na Zhao, Kai Zhao, Han Zhang, Jiangyu Sheng, Shasha Feng, Wei Wang*

*School of Chemistry and Chemical Engineering, Lanzhou Jiaotong University, Lanzhou 730070, China*

---

* Corresponding author, e-mail: wangwchem@163.com, wangw@mail.lzjtu.cn (W. Wang)

## 1. Materials

Modified epoxy acrylate (YC1181) purchased from Shanghai Yinchang New Materials Co., LTD. Butyl acrylate (AR) was purchased from Shanghai Maclin Biochemical Technology Co., LTD. Soluble starch (AR) was purchased from Yantai Shuangshuang Chemical Co., LTD. Phosphorous oxide (97 %) was purchased from Aladdin Reagent Factory. $NH_4Cl$ (AR) was purchased from Tianjin BASF Chemical Co., LTD. $C_2H_5OH$ (AR) is purchased from Aladdin Reagent Factory. $KHCO_3$ (AR) was purchased from Sahn Chemical Technology (Shanghai) Co., LTD. Liet-C (AR) was purchased from Sigma Aldrich (Shanghai) Trading Co., LTD. Graphite paper (AR) purchased from the new material of Tankan Lang Co. LTD. $C_{18}H_{15}P$ (99 %) purchased from Vasili Chemical. All reagents are used without further purification. $N_2$(>99.999 %), Ar(>99.999 %), $CO_2$ (>99.999 %) and compressed air (>99.999 %) were purchased from Lanzhou Yulong Gas Co., LTD. Standard gas ($H_2$, CO, $CH_4$, $N_2$) (mixture) was purchased from Dalian Date Gas Co., LTD.

## 2. Preparation of the electrocatalysts

### 2.1. Preparation of 3D printing ink

Based on the mass number, 40 parts modified epoxy acrylate, 60 parts butyl acrylate and 20 parts soluble starch were mixed, stirred for 4 hours, and then added 4 parts photoinitiator (diphenylphosphine oxide), continuously stirred for 1 hour, so that the solution became uniform, and the 3D printing ink was prepared.

### 2.2. 3D printing process

Firstly, the ideal electrode structure was designed by computer software (3D

Max) and the required 3D models were established. The 3D-printed electrode precursor models designed in this work were a snowflake shape with dimensions of 1.8*1.8*0.5 cm and a seven-membered ring with dimensions of 2.0*2.0*0.5 cm, and then the model was converted into STL file format by the light curing 3D printer software. Then, the model is "sliced" with the Photon software, converting the entire 3D model into a large number of 2D cross-sectional layers. After it, the model is converted into a G-code file. Finally, the 3D printer sequentially prints a large number of cross-sectional layers from bottom to bottom until the desired 3D component is finished. During the printing process, the printer's exposure time is set to 16 seconds and the slice thickness is 0.05 mm.

### 2.3. Preparation of catalytic electrode

The 3D printed precursor converted into the phosphate nitrogen-codoped catalytic electrode (3Dp-PNCE) can be divided into the following steps. First, to strengthen the mechanical stability of the printed precursor body, it is placed under the ultraviolet curing lamp for 1 hour on both sides, and then freeze-dried at -50 ℃ for 24 hours. After that, the printed precursor body was placed in a 20 mL supersample bottle, with ultra-pure water as the solvent, $NH_4Cl$ (200 g $L^{-1}$) and different triphenylphosphine (6, 8, 10, 12, 14 g $L^{-1}$) as the doping agent, ultrasound treating for 4 hours to make those chemicals fully enter the printed precursor body. Finally, it is treated with high temperature under argon atmosphere (at the rate of 3 ℃ $min^{-1}$ to 300 ℃, constant temperature for 1 hour, and then heated to different temperatures (850, 900, 950, 1000, 1050 ℃) for 1 hour). Meanwhile, the 3D printed self-supporting carbon electrode without $NH_4Cl$ and triphenylphosphine is called 3Dp-CE reference.

## 3. Electrochemical measurements

The 3Dp-PNCE prepared by photocuring 3D printing technology was used for electrocatalytic carbon dioxide reduction, and the electrochemical performance was tested by CHI electrochemical workstation.

The catalytic electrode was glued to graphite paper (thickness 0.025 mm) with conductive adhesive (Leit-C) and then soaked in 0.1 M $KHCO_3$ (pH = 6.8) for 1 hour. Finally, the catalytic electrode is clamped onto the electrode clamp. The electrolysis test device is a three-electrode system. The obtained catalytic electrode is the working electrode, while the saturated calomel electrode and the platinum mesh electrode are the reference electrode and the opposite electrode, respectively. The cathode chamber and anode chamber of the H-type electrolytic cell are separated by a proton exchange membrane (Nafion 117), and the electrolyte is 0.1 M $KHCO_3$. Before the electrolysis test, high-purity $CO_2$ was injected into the cathode chamber at a flow rate of 24 mL $min^{-1}$, and electrolysis began after continuous injection for 30 min. In addition, when performing impedance tests, the three-electrode system is installed in a single-port electrolytic cell, and the reference electrode is replaced with the Ag / AgCl electrode, and the electrolyte is consistent with the electrochemical performance test. All potentials in the study are converted into reversible hydrogen electrode values (*vs.* RHE).

The gas products produced by electrolysis were analyzed by gas chromatograph and the standard gas chromatographic curves of CO and $H_2$ at different concentrations were drawn. CO and other hydrocarbons are detected by a flame ionization detector (FID), while $H_2$ is detected by a thermal conductivity detector (TCD). After electrolysis, nuclear magnetic resonance spectrometer was used to detect the electrolyte in the cathode chamber. 5 μL internal standard (acetonitrile) was mixed with 5 mL $D_2O$ to form mother liquor, and then the mother liquor was diluted 20 times with $D_2O$, and then the diluted mother liquor was mixed with 400 μL cathode chamber electrolyte, and the liquid phase products were analyzed by Nuclear Magnetic Resonance.

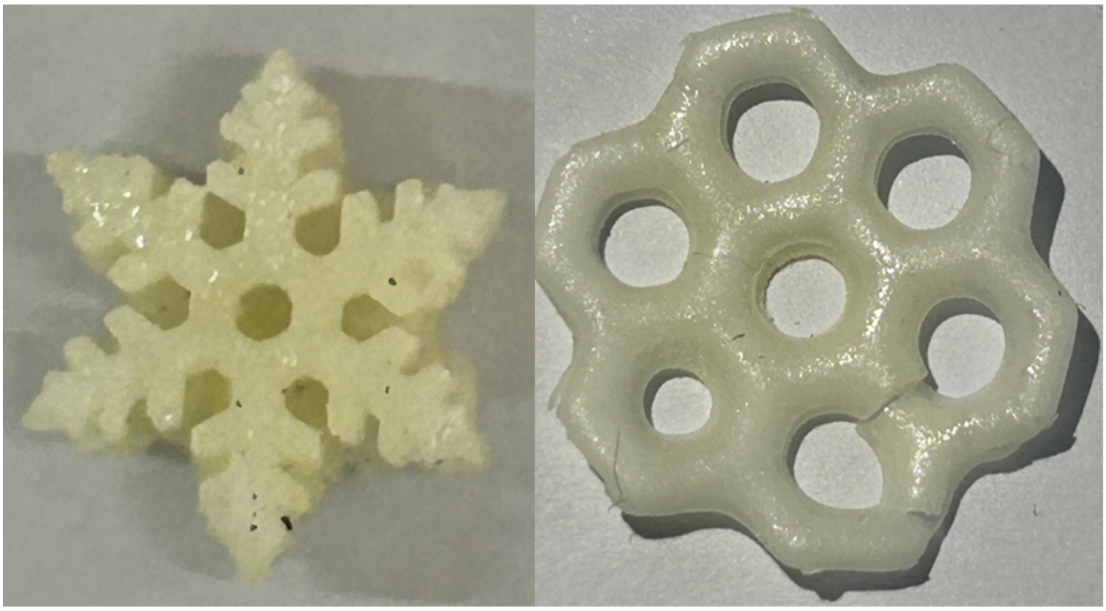

**Fig. S1** 3D printed precursor with different shapes.

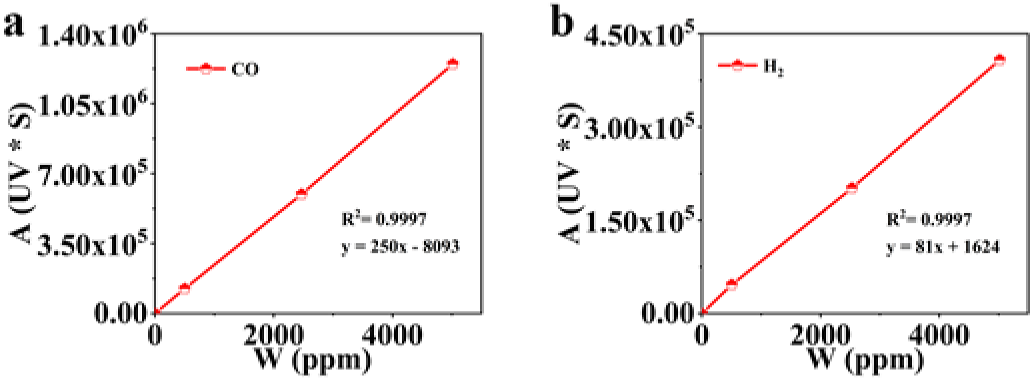

**Fig. S2** Gas Chromatographic Standard Curves of CO (a) and $H_2$ (b) at Different Concentrations.

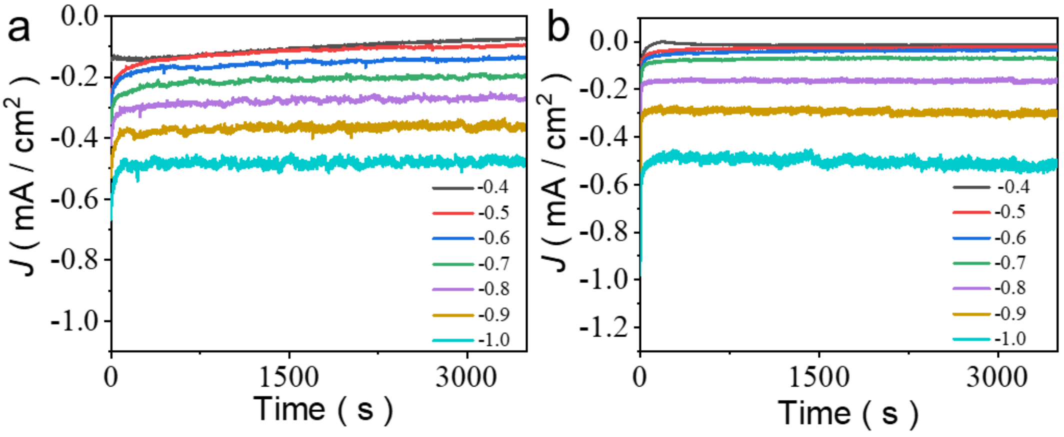

**Fig. S3** The optimal 3Dp-PNCE (a) and 3Dp-CE (b) in terms of current density at different potentials.

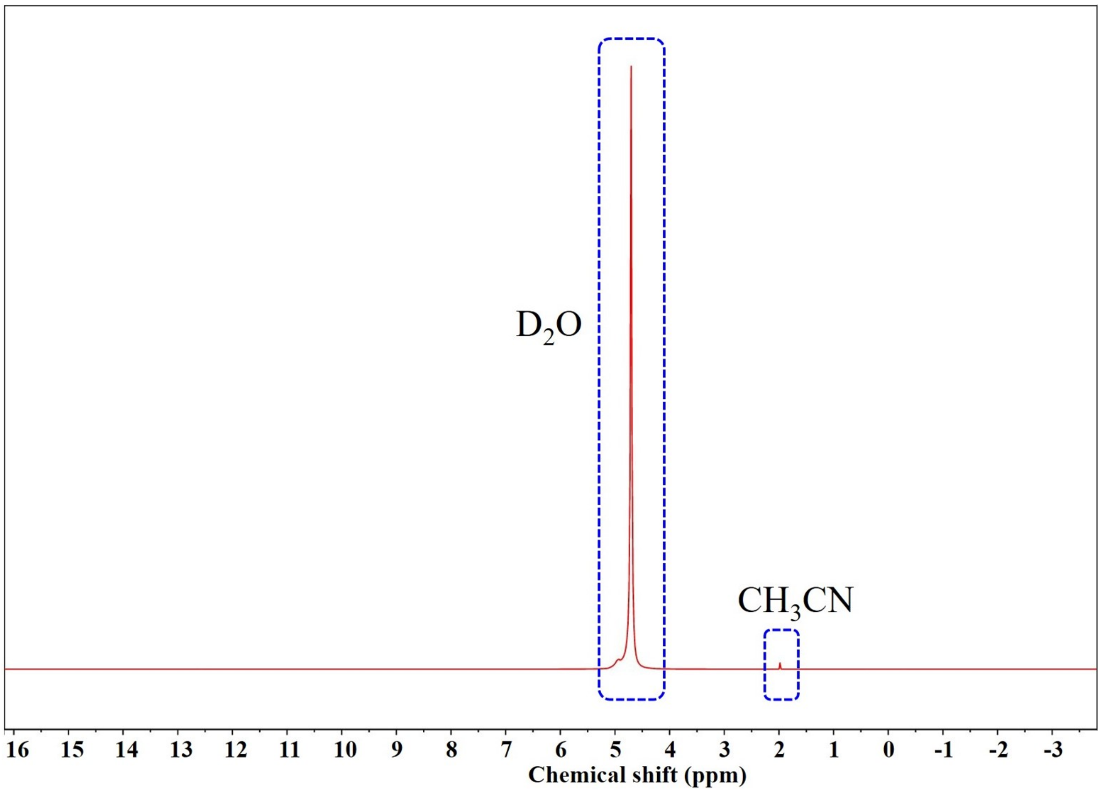

**Fig. S4** Representative $^1$H NMR spectra of the electrolyte after 10 h of electrolysis on the optimal 3Dp-PNCE.

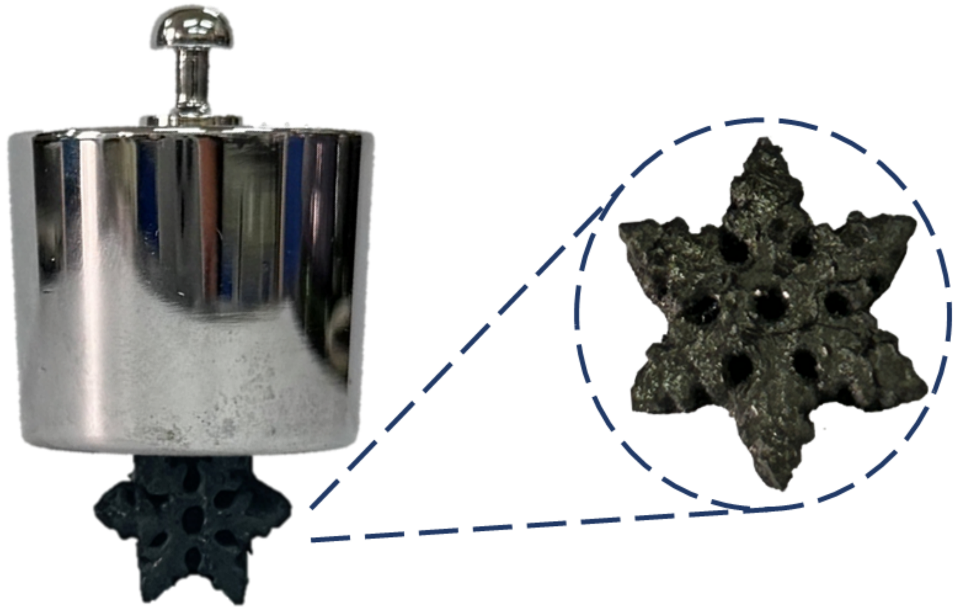

**Fig. S5** The optimal 3Dp-PNCE was subjected to a mechanical stability test under a 100 g load.

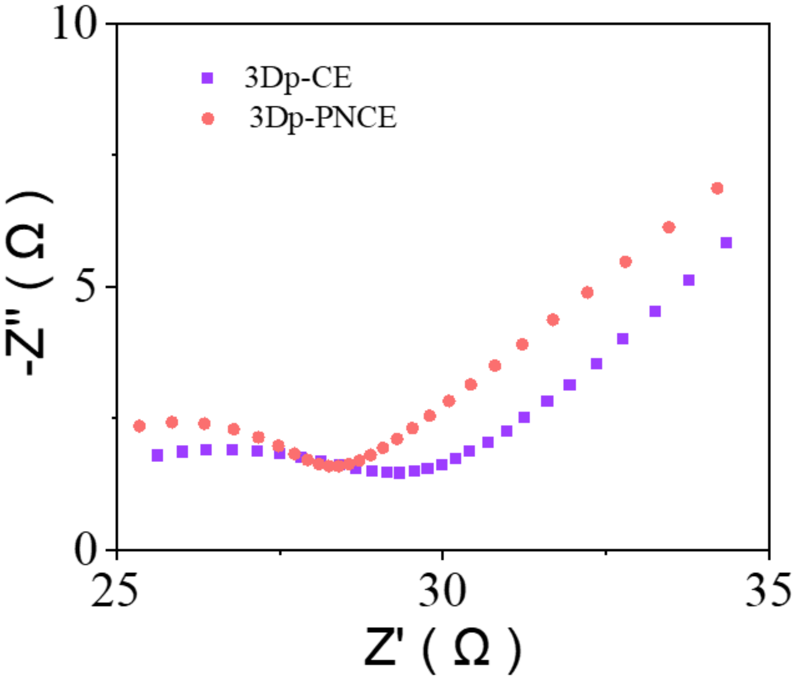

**Fig. S6** Nyquist diagram of the optimal 3Dp-PNCE and 3Dp-CE.

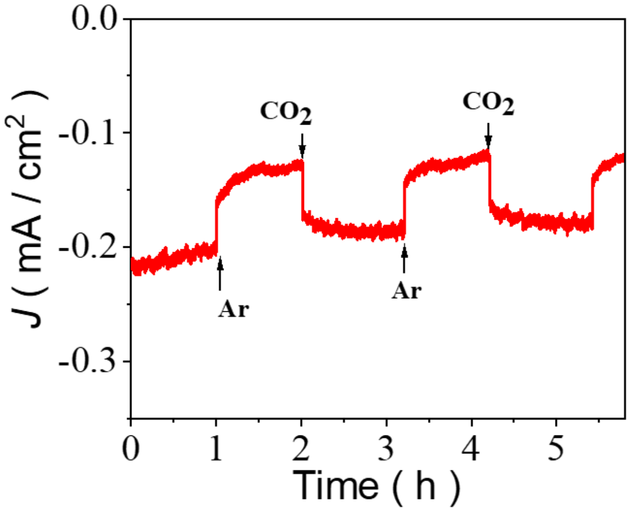

**Fig. S7** Ar and $CO_2$ exchange intake test at -0.7 V on the optimal 3Dp-PNCE.

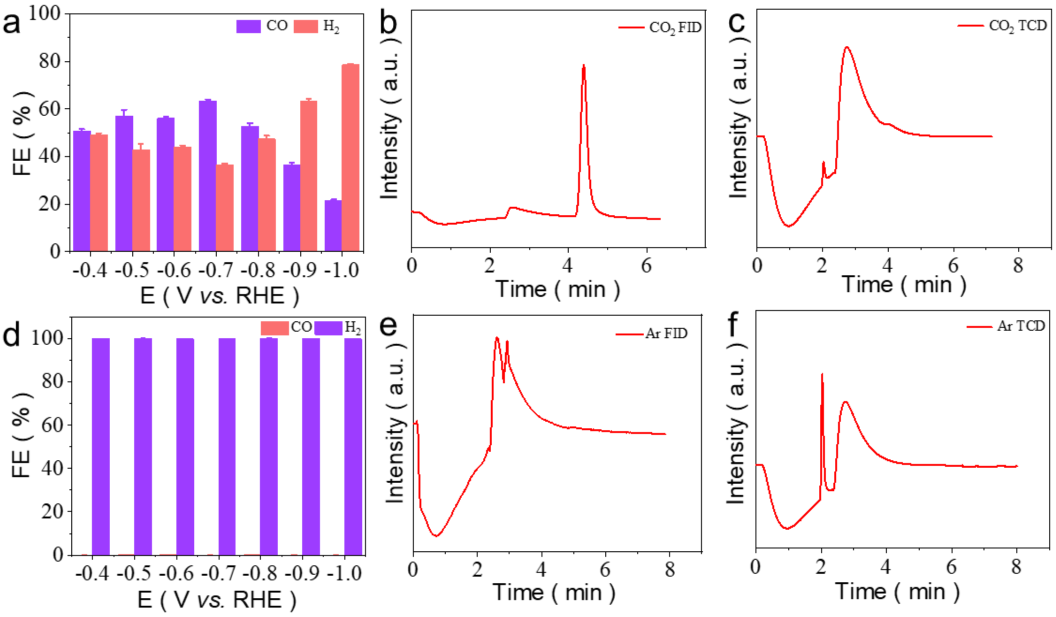

**Fig. S8** Gas chromatogram of FE (a) with $CO_2$ as feed gas and corresponding FID detector (b) and TCD detector (c) on the optimal 3Dp-PNCE; Gas chromatogram with Ar as feed gas for FE (d) and corresponding FID detector (e) and TCD detector (f) on the optimal 3Dp-PNCE.

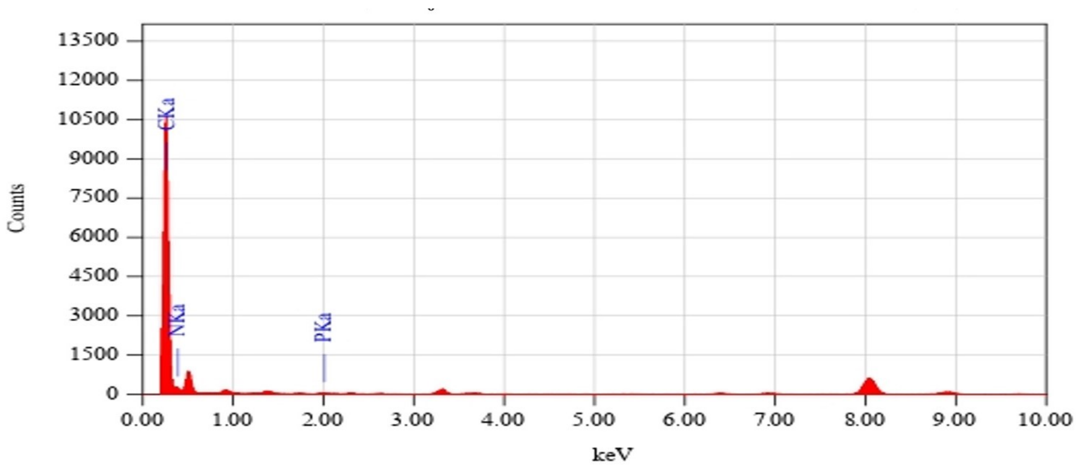

**Fig. S9** EDX spectrum of on the optimal 3Dp-PNCE.

**Tab. S1** Comparison of 3Dp-PNCE with other catalytic electrodes in previous reports.

| **materials** | **Does it involve 3D printing** | **Is it metal-free** | **Application** | **Ref.** |
|---|---|---|---|---|
| **3Dp-PNCE** | **Yes** | **Yes** | **$CO_2RR$** | **This work** |
| 3D hp CuAg | Yes | No | Tunable $CO_2$ Reduction to Syngas | 1 |
| Ni@NCNT/CM | No | No | $CO_2RR$ | 2 |
| Ni, N-C | No | No | $CO_2RR$ | 3 |
| 3D-CE-NiFe | Yes | No | $CO_2RR$ | 4 |
| Cu@Sn NWs | No | No | $CO_2RR$ | 5 |
| Cu-based nanocatalysts | No | No | $CO_2RR$ | 6 |
| FePc/MXene | No | No | $CO_2RR$ | 7 |
| PcCu-based 2D MOF | No | No | $CO_2RR$ | 8 |
| Se-BP-N-C | No | Yes | $CO_2RR$ | 9 |
| mp-Ni-N-Cs | No | No | $CO_2RR$ | 10 |

**Tab. S2** The performance comparison of 3Dp-PNCE with other catalytic electrodes.

| materials | Potential(V) | Ratio of $H_2$:CO | Electrolytes | Ref. |
|---|---|---|---|---|
| **3Dp-PNCE** | **-0.40~-1.00 (*vs.* RHE)** | **0.58~3.65** | **0.1 M KHCO3** | **This work** |
| $Cu_{0.5}Cd_{0.5}$-O | -0.56~-1.16 (*vs.* RHE) | 9.25 | 0.5 M $KHCO_3$ | 11 |
| AuZn@ZnO | -0.70~-1.10 (*vs.* RHE) | 0.25~2.5 | 0.1 M $KHCO_3$ | 12 |
| $Ag/TiO_2$ | -0.30~-0.70 (*vs.* RHE) | 0.10~1.50 | 1 M $KHCO_3$ | 13 |
| R-$Ag/TiO_2$/p-Si | -0.20~-0.90 (*vs.* RHE) | 0.33~1.00 | 0.1 M $KHCO_3$ | 14 |
| CoNC-400 | -2.00~-2.60 (*vs.* $Fc/Fc^+$) | 0.94~1.18 | acetonitrile solution | 15 |

## Supplementary references

1 W.Y. Yan, C. Zhang and L. Liu, *ACS Appl. Mater. Interfaces,* 2021, **13**, 45385-45393.

2 S.J. Shen, C. Han, B. Wang and Y.D. Wang, *Adv. Mater. Interfaces*, 2021, **8**, 2101542.

3 X.Y. Tan, C. Yu, S. Cui, L. Ni, W. Guo, Z. Wang, J.W. Chang, Y.W. Ren, J.H. Yu, H.L. Huang and J.S. Qiu, *Chem. Eng. J.*, 2022, **433**, 131965.

4 Jiangyu Sheng, Mingshu Gao, Na Zhao, Kai Zhao, Yaoan Shi and Wei Wang, *Fuel*, 2025, **382**, 133703.

5 X.D. Lv, J.Y. Liu, T. Shao, M. Ye and S.W. Liu, *Catal. Today*, 2023, **420**, 114188.

6 H. Xie, T.Y. Wang, J.S. Liang, Q. Li and S.H. Sun, *Nano Today*, 2018, **21**, 41-54.

7 M. Gao, Y. Sun, K. Zhao, M. Zhang, X. Wang and W. Wang, *J. Environ. Chem. Eng.*, 2024, **12**, 111802.

8 S. Osella and W.A. Goddard, *J. Am. Chem. Soc.*, 2023, **145**, 21319-21329.

9 Y. Sun, K. Zhao, X.M. Deng, M. Zhang, X.L. Wang and W. Wang, *J. Environ. Chem. Eng.*, 2023, **11**, 110435.

10 W. Wang, K.Y. Chen, Y. Sun, S.Q. Zhou, M. Zhang and J.Y. Yuan, *Appl. Mater. Today*, 2022, **29**, 101619.

11 C. Wang, X. Hu, B. Chen, H. Ren, X. Wang, Y. Zhang, X. Chen, Y. Liu, Q. Guan and W. Li, *J. Energy Chem.*, 2024, **91**, 50-58.

12 R. Zhao, Z.Y. Zhu, T. Ouyang and Z.Q. Liu, *Angew. Chem. Int. Edit.*, 2024, **63**, e202313597.

13 Y.E. Kim, B. Kim, W. Lee, Y.N. Ko, M.H. Youn, S.K. Jeong, K.T. Park and J. Oh, *Chem. Eng. J.*, 2021, **413**, 127448.

14 C. Kim, S. Choi, M.-J. Choi, S.A. Lee, S.H. Ahn, S.Y. Kim and H.W. Jang, *Appl. Sci.*, 2020, **10**, 3487.

15 X. Zhang, F.C. Romeiro, S.X. Guo, Y. Zhang, E. Nossol, R.C. Lima, A.M. Bond and J. Zhang, *Chemelectrochem*, 2019, **6**, 1508-1513.